HEFAT2010
7th International Conference on Heat Transfer, Fluid Mechanics and Thermodynamics
19-21 July 2010
Antalya, Turkey

VASCULAR DESIGN FOR COMPACTNESS: TRANSIENT VOLUMETRIC COOLING

S. Lorente[1] and A. Bejan[2]*
[1]Université de Toulouse; INSA; Laboratoire Materiaux et Durabilite des Constructions;
135, avenue de Rangueil; 31 077 Toulouse Cedex 04, FRANCE
[2] Duke University; Department of Mechanical Engineering and Materials Science
Durham, North Carolina 27708-0300, USA
*Author for correspondence: abejan@duke.edu

ABSTRACT

The drive toward greater cooling densities in generating an entirely new literature on *vascular designs*: tree-shaped flow architectures that offer dramatically superior volumetric functionalities for smart materials, such as volumetric cooling, self-healing and functionally graded material properties. In this paper we review our group's progress with the *constructal design* of dendritic flow architectures for cooling. We describe the development of cooling architectures consisting of trees. Such vasculatures provide volumetric bathing for a slab with flow entering from one side and exiting through the other side. The volumetric generation rate is uniform. The volume fraction occupied by all the channels is fixed, as a consequence of the fact that the leading constraints on high-density design are fixed weight (solid volume) and fixed volume (solid and channel volume). Minimized are the global thermal resistance (or hot-spot temperature), the global fluid flow resistance, and the volume fraction of material with temperatures close to the hot-spot temperature. For steady state operation, we show that there is an architecture with a certain number of bifurcation levels that meets the multiple objectives. Unsteady state performance is also provided by the dendritic designs. A time delay separates the sensing of overheating from the start of the flow of coolant. The longest time delay that allows the vasculature to keep all the temperatures below the permissible level is reported as a function of the complexity of the tree architecture.

Keywords: Constructal; vascular; compactness; dendritic flows; tree-shaped flows.

INTRODUCTION

The development of multifunctional smart materials calls for vascularization: the design of intricate flow architectures that distribute fluids through the entire volume of the material. These developments are part of the current movement of the frontier in thermal sciences, toward compactness, distributed energy systems, and designs that resemble living tissues and organs [1]. The current literature is showing these trends in new articles on the properties, design and performance of tree-shaped flow architectures.

Trees are the effective way to guide flows from discrete points to continua (curves, areas, volumes), and vice versa. The fluid-flow performance of complex trees is superior to that of parallel channels. This body of work is coming together as constructal theory, which is the view that the generation of flow configuration in nature is a physics phenomenon, in which freely morphing flow systems evolve in time as a sequence of easier flowing configurations [2].

New vascular materials have new properties that must be determined. Here we review our group's most recent work on the transient response of a vascular body subjected to sudden heating and fluid flow [3-5]. We illustrate this fundamental problem in the three-dimensional slab configuration shown in Fig. 1. At the time t = 0, heat is generated uniformly over the area at the rate q''. The larger three-dimensional body can be a stack of many such slabs, so that the surface heating for one slab is a model for the volumetric heating through the larger volume. The coolant starts flowing at $t = t_d$, and sweeps the area from side to side. The vasculature for this sweep consists of trees that alternate with upside down trees, in accordance with the line-to-line trees proposed in Ref. [6], where it was shown that the advantage of line-to-line trees in comparison with transversal parallel channels is that they offer a smaller global flow resistance when the smallest length scales are small enough so that the number of pairing levels in the tree structure is greater than 4.

GEOMETRY

The geometrical features of the flow architecture are defined in Fig. 1. Each tree is designed in accordance with the minimal-lengths tree design proposed in Ref. [7], which yielded 90^o angles at every bifurcation level. Although the minimal-lengths trees are approximate (near optimal), their fluid flow performance comes surprisingly close to that of the fully

optimized tree architectures. For example, the global flow resistance of a minimal-lengths tree with fully developed laminar flow and one level of pairing (i.e. a construct shaped as "Y") exceeds by only 0.5 percent the global flow resistance of the fully optimized Y construct [6].

Because of the 90° angles, the outer branch of every bifurcation is collinear with the stem. The asymmetry of the Y shape makes the splitting of the stream unequal, with more fluid flowing along the collinear paths. This flow imbalance becomes more accentuated when the svelteness of the architecture Sv is less than 10, because in this domain the local pressure losses (junctions, bends, entrances) are not negligible. The svelteness is a global geometric property of the architecture, which is defined as [8],

$$\mathrm{Sv} = \frac{\text{external flow length scale}}{\text{internal flow length scale}} = \frac{\mathrm{Y}}{\mathrm{V_c^{1/3}}} \qquad (1)$$

where V_c is the total volume of the flow channels. Worth noting is that the flow imbalance downstream from a bifurcation is beneficial for convective cooling, because with larger flow rates through the outer channels of each bifurcation the tree is more effective in convecting away the heat generated by the larger subvolumes residing on the outer sides of the outer channels (e.g., the area labeled "A" in Fig. 1).

The lengths of all the channels in a line-to-line tree with p pairing levels are

$$L_i = 2^{p-i-1/2}d, \quad (i = 0, 1, ..., p) \qquad (2)$$

where d is the spacing between two adjacent ports of the tree canopy. In every natural or manufactured structure, there is a length scale that is the smallest, for example, the alveolus in the lung, and the spacing between the smallest fins in the most compact heat exchanger [2, 9]. Here that smallest detail is d, and it is the length scale visible from the outside of the vascularized slab. The smallest length scale is specified. The

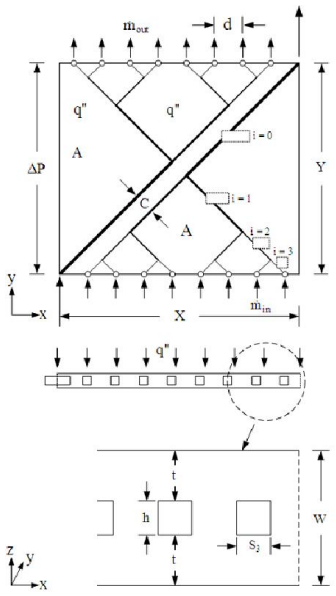

Figure 1 Line-to-line tree architecture, as a sequence of point-to-line trees alternating with upside down trees [3].

Table 1. The design domain $\mathrm{Sv}(p, \phi)$ in which the channels of the two trees of Fig. 1 do not interfere. The numbers listed in the table indicate the value of the slenderness number Sv [3].

p	ϕ					
	0.005	0.01	0.02	0.03	0.04	0.05
1	9.0	7.1	5.6	4.9	4.5	4.2
2	12.0	10.3	8.2	7.1	6.5	6.0
3	17.4	13.8	10.9	9.6	8.7	8.1
4	22.7	18.0	14.3	12.5	11.3	10.5
5	29.0	23.0	18.3	16.0	×	×
6	36.8	29.2	×	×	×	×
7	×	×	×	×	×	×

length of the tree in the flow direction is Y, Fig. 1. The thickness of the vascularized conducting body (W) scales with d. In this example we set W = d/4 = 1.25 mm, as shown in Table 1. The distance between two adjacent trees (C) is also comparable with d. The design of the layout must be executed with care so that tree-tree interference $(C < 0)$ is avoided.

The number of channels of the same size in a single tree is $n_i = 2^i$, (i = 0, 1, …, p). The channel cross-sections are rectangular, $h \times S_i$, Fig. 1. The manufacturing of such channels is easier when all the channels have the same depth (h). The channel widths (S_i) are selected based on a very effective rule derived from the classical Hess-Murray rule for bifurcation round tubes of diameters $D_i > D_{i+1}$ [1]:

$$\frac{D_i}{D_{i+1}} = 2^{1/3} \qquad (3)$$

Written in terms of tube cross-sectional areas ($A_i = \pi D_i^2/4$), the Hess-Murray rule is

$$\frac{A_i}{A_{i+1}} = 2^{2/3} \qquad (4)$$

Rule (4) is adopted in the present design, and, because $A_i = hS_i$ with h = constant, this rule yields the sequence of rectangular channels widths,

$$\frac{S_{i+1}}{S_i} = 2^{-2/3} = 0.63 \qquad (5)$$

Because the best of all rectangular cross-sections is the square, the shape chosen for the smallest cross-sections of the canopy (i = p) is square. This is the shape of the small ports through which the tree canopy communicates with the outside (Fig. 1, bottom). The stream-wise and transversal length scales of one tree are (cf. Fig. 1)

$$X = \left(2^p + \frac{1}{2} \right) d \,, \quad Y = \left(2^p - \frac{1}{2} \right) d \,, \tag{6}$$

which means that when p is large the X × Y domain is almost square. The thickness of the thinnest wall of solid material is t, which means that the third dimension of the slab is

$$W = h + 2t \tag{7}$$

The total volume occupied by channels,

$$V_c = 2 \sum_{i=0}^{p} 2^i S_i h L_i \tag{8}$$

is used for calculating the svelteness Sv, Eq. (1), and the effective porosity of the vascularized body

$$\phi = \frac{V_c}{V} \tag{9}$$

where the total volume is V = XYW.

We studied many configurations, which can be imagined to populate a design space with dimensionless coordinates such as ϕ, p, Sv, etc. For illustration, the presentation is made in dimensional terms, with d = 0.5 cm as the reference length scale. The dimensions of the elemental tree (X × Y) increase as the number of pairing levels p increases. This is suggested qualitatively in Fig. 2, where one should imagine that d has the same size in all four drawings.

Because the channels have finite widths (Fig. 2), complex tree structures are possible only if ϕ is sufficiently small. The criterion for avoiding interference between adjacent trees is $(S_0/S_1)/2 < C$, for which the spacings S_0 and S_1 are defined in Fig. 1. Based on this criterion we constructed Table 1, which shows the design domain (p, ϕ, Sv) that we have explored, and the domain that is not accessible (indicated by ×). The table also shows the svelteness of each (p, ϕ) tree structure. The fact that Sv is not much greater than 10 means that pressure losses at the junctions are not negligible, and that full numerical simulations of the flow were necessary in order to capture the details of the flow and pressure losses at all the junctions. The upper dashed line corresponds to Sv ~ 10, indicating that the cases shown in the upper-right of the table (small p, large ϕ) are expected to have significant local pressure losses.

NUMERICAL MODEL

The numerical model is based on assuming unsteady, incompressible laminar flow in every channel, and constant properties for the solid and the fluid. Details of the numerical approach are given in Refs. [3-5]. The global thermal resistance was nondimensionalized as

$$\tilde{R}_{max} = \frac{T_{max} - T_{min}}{q'' Y^2 / (k_s W)} \tag{10}$$

where T_{max} and T_{min} are the hot spot temperature and the inlet temperature of coolant, respectively. The corresponding dimensionless temperature distribution is represented by

$$\tilde{R} = \frac{T - T_{min}}{q'' Y^2 / (k_s W)} \tag{11}$$

where T(x,y,z) is the local temperature anywhere in the vascularized volume. Because the heat transfer rate is fixed, the global resistance $\tilde{R}_{max}$ is a dimensionless measure of the excess temperature registered in the hottest spots of the system.

TRANSIENT CONJUGATE HEAT TRANSFER

The heat and fluid flow in the vascularized material was simulated as a conjugate conduction and convection phenomenon that covers continuously the entire three-dimensional vascularized volume. The simulations were performed for structures with p = 1, 2, 3 and 4, as illustrated in Fig. 2. The porosity was $\phi = 0.02$ in all cases. The ratio of thermal conductivities k_s/k_f emerges as a dimensionless parameter in the dimensionless formulation of conjugate heat transfer because of the continuity of heat flux across solid-fluid interfaces. The value $\tilde{k} = 24$ was chosen because it corresponds to the solid-fluid combination of stainless steel (AISI 304) and liquid water at ambient conditions.

The pressure difference imposed from side to side was fixed by specifying the Bejan number proposed by Bhattacharjee and Grosshandler [10] and Petrescu [11],

$$Be = \frac{\Delta P \cdot Y^2}{\alpha_f \mu_f} \tag{12}$$

where α_f and μ_f are the thermal diffusivity and viscosity of water. The Be range was 10^8-10^{12}, which corresponds to laminar flow in all the channels (Re < 1000). Figure 3 shows the global thermal resistance versus Be in the steady-state results, i.e. as the time increases indefinitely, $t \to \infty$. The resistance curves have an apparent envelope along which the minimum global thermal resistance decreases as the available Be increases. The intersections between two consecutive designs (p and p + 1) are points where the designer has a choice. At the intersection between p = 1 and p = 2, there is a 1 percent difference between the global thermal resistances of the two designs.

TIME DELAY BEFORE THE START OF COOLING

In the simulations of transient conjugate heat transfer it was assumed that the fluid flow is in the steady-state, and that its inlet bulk temperature is fixed at T_{min}. The initial temperature

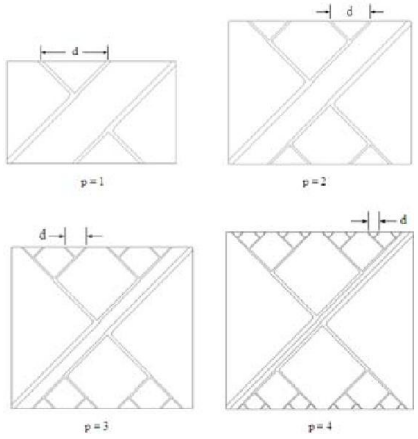

Figure 2 Line-to-line tree architectures with one, two, three and four levels of pairing [3].

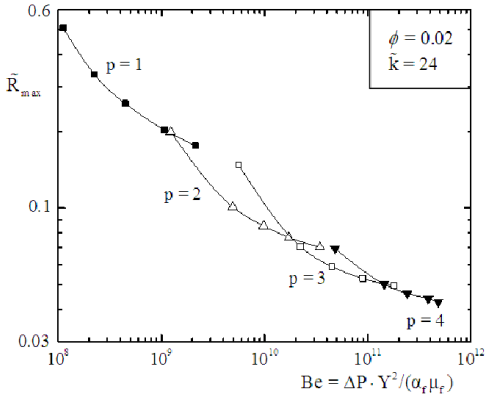

Figure 3 Numerical results for global thermal resistance versus pressure drop number (Be) under steady-state condition in the structures of Fig. 2 [3].

of solid slab is also T_{min}. At $t = 0^+$ the uniform heat flux q'' lands uniformly on the X × Y surface in Fig. 1, i.e., perpendicularly to the direction of fluid flow. The Y sides of the computational domain are planes of symmetry. The X sides and the bottom surface X × Y are adiabatic.

In practice, the implementation of smart vascular materials with self-cooling also requires a system of sensing the start of heating, so that the flow of coolant can begin. A time delay t_d separates the start of heating and the start of convection cooling. At t = 0, the uniform heat flux q'' is applied on a slab that is not bathed by coolant (the tree channels are filled with stagnant coolant) and all the remaining external surfaces are adiabatic. At $t = t_d$, the coolant starts to flow in steady fully developed fashion.

First, we determined another characteristic time of the vascular system – the thermal inertia time t_c, as shown in Fig. 4. If the coolant is not flowing, then shortly after t = 0 the peak temperature of the system increases almost linearly in time. The system is also characterized by its steady-state peak temperature indicated by $\tilde{R}_{max,\,ss}$, which occurs late enough

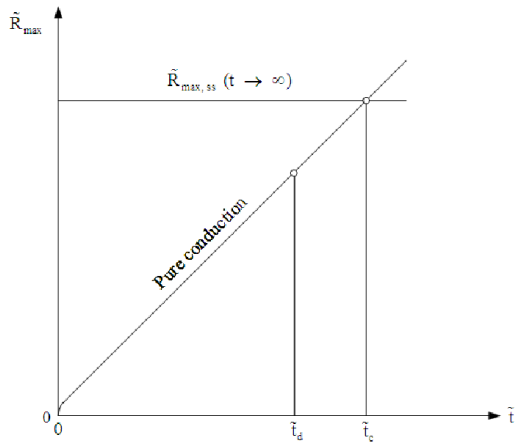

Figure 4 Definition of the thermal-inertia time constant of the vascular system [3].

when coolant is flowing. The intersection of the two lines defines the thermal inertia time $\tilde{t}_c$. The time delay before the start of the flow of coolant ($\tilde{t}_d$) is selected relative to $\tilde{t}_c$, as a fraction of the thermal inertia time,

$$\tau = \frac{\tilde{t}_d}{\tilde{t}_c} \tag{13}$$

In Fig. 5 we investigated the effect of τ on the transient response of the vascularized body. When the delay time τ is larger than a critical value (called τ_*), the peak temperature overshoots the steady-state level. The overshoot must be avoided so that the peak temperature worthiness of the vascular design continues to be described by the steady-state peak temperature. Furthermore, the critical time delay τ_* is a valuable feature to know because it represents the longest delay time within which the vascular design is still safe to operate without coolant flowing.

We performed many time-dependent simulations and the results for τ_* are summarized in Fig. 6. The τ_* values decrease as the pairing level (p) increases. For p = 1 and p = 2,

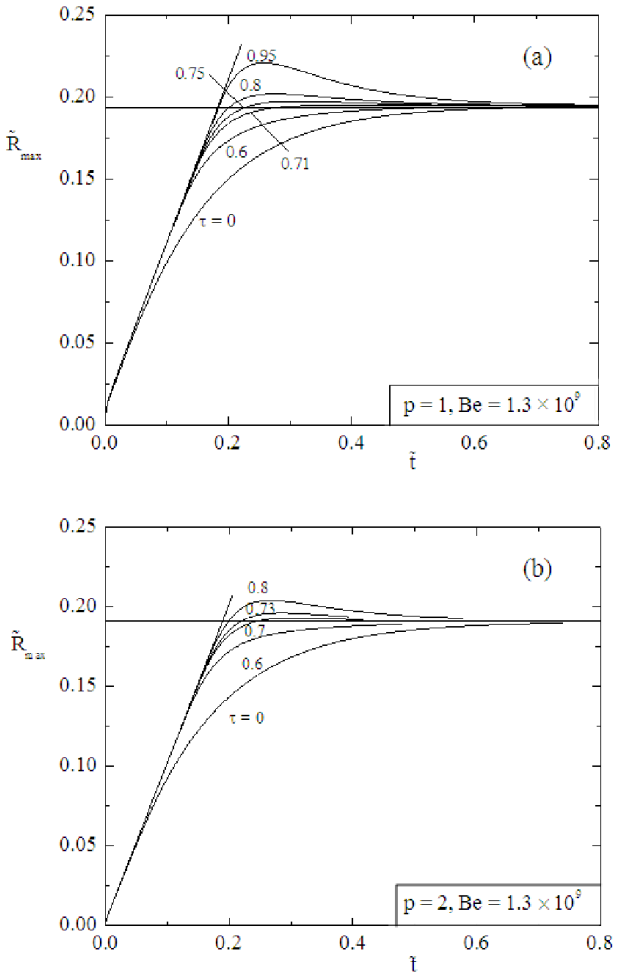

Figure 5 The effect of the coolant time delay on the evolution of the peak temperature for the first design transition (p = 1, 2). (a) p = 1, (b) p = 2 [3].

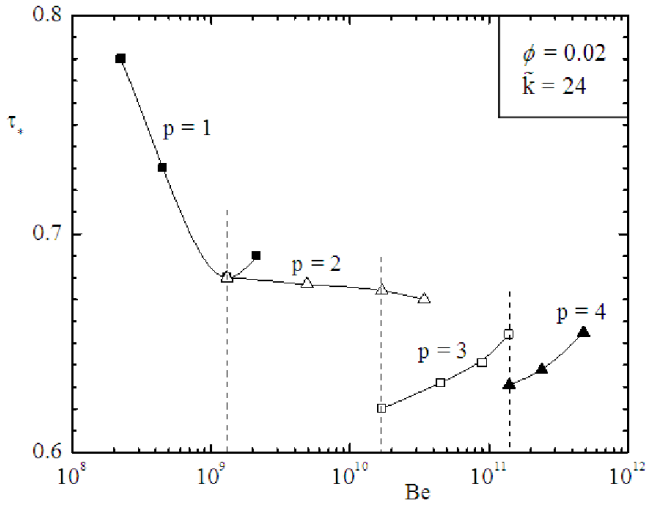

Figure 6 Critical time delay (τ_*) versus Bejan number (Be) [3].

they decrease as Be increases. For p = 1 the critical time increases slightly when Be is greater than that of the first intersection. This means that the design with p = 1 has the smallest critical time in the vicinity of the first design intersection. For p = 3 and p = 4, the τ_* values increase as Be increases. The chart of τ_* vs. Be (Fig. 6) does not mimic smoothly the trend exhibited in Fig. 3.

SUDDEN HEATING IN COUNTERFLOW WITH THE VASCULATURE

An alternative configuration is shown in Fig. 7 [4]. The solid wall of thickness L that is heated with uniform heat flux q'' from the left side. The right side is insulated. The wall is cooled by a single-phase fluid driven by a specified pressure difference ΔP. The wall has many elemental volumes of the kind shown in Fig. 7. All the channels are round, and the diameters of the channels are sized relative to one another in accordance with the Hess-Murray law. The thickness of the element in the direction perpendicular to the figure is set equal to the spacing d. The vertical dimension H of one element is 2^{p+1}d, where p is the number of pairing levels (e.g., p = 3 in Fig. 7). Several volume elements stacked in the vertical direction in Fig. 7 constitute a slab vascularized with line-to-line tree structures. In the present study we conducted simulations for structures with p = 1, 2, 3 and 4.

The porosity was fixed at ϕ = 0.05. By "porosity" we mean the volume fraction occupied by all the channels. The vascular structure is not porous medium in the usual sense; yet, its volume fraction is fixed, for two reasons. Most applications of vascular designs for self-cooling are projected for future vehicles (e.g. aircraft). In such applications, the mass of the structure (mostly solid mass) is fixed, and so is its volume (solid and fluid). These mass and volume constraints translate into a fixed ϕ value.

The time-dependent evolution of the flow and temperature fields has two distinct time intervals. In the first, the coolant is assumed to flow steadily due to the imposed pressure difference

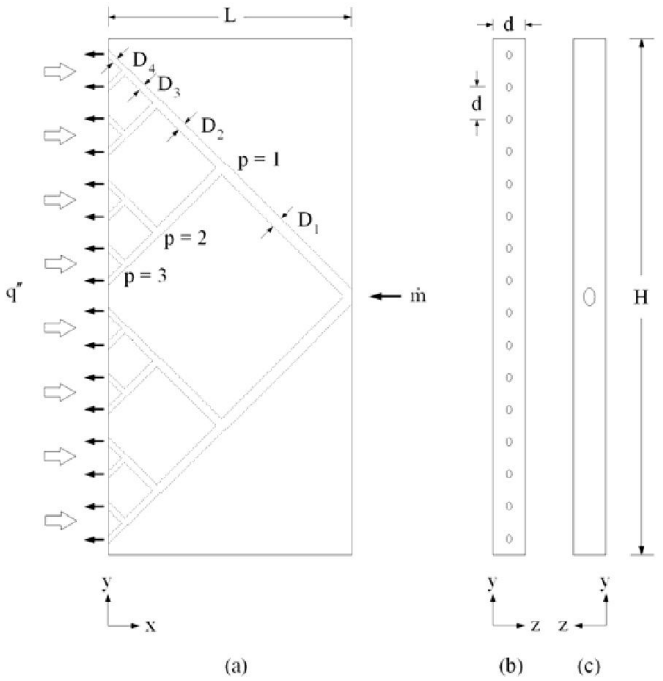

Figure 7 Tree-shaped flow structure with three levels of bifurcation: (a) The mid plane of the flow element; (b) The view from the left, showing the outlets; (c) The view from the right, showing the inlet [4].

Be, before heating is imposed from the side. The purpose of the simulation of this first interval is to find the thermal response of the vascularized wall, and to compare it with the thermal response of a solid wall without channels (ϕ = 0).

The second time interval follows after heating is imposed. In practical applications a sensor detects the heating, after which an actuator pumps the coolant. There is an unavoidable time delay (t_d) between sensing and actuating. The objective is to determine the longest allowable delay such that the vascular body does not overheat.

The initial conditions are (1) the temperature is uniform over the entire system, at the lowest level (coolant inlet temperature, T_{min}), and (2) the fluid flow is steady and driven by the pressure difference Be. At the time $t = 0^+$, the left side of the wall is exposed to the heat flux q''. Throughout this work we monitored the highest temperature ($\tilde{T}_{max}$), not the locations where the hot spots occur. It is important to note that the locations change as the parameters change (Be, p), and as time increases.

The allowable time delay is determined by two factors. One is how fast the vascularized wall is cooled by the coolant, and this is associated with the characteristic response time. The other accounts for how fast the peak temperature rises during the delay, when there is no coolant. If the peak temperature increases slowly during the delay, and responds fast after the coolant starts flowing, then the allowable time delay is long, which is an attractive feature in design (robustness). In order to evaluate the second factor, we define the thermal inertia time, or time constant $\tilde{t}_c$, which is the time when the hot-spot

temperature reaches the steady-state hot-spot temperature in the absence of coolant,

$$\tilde{T}_{max,\,no\ flow}\left(\tilde{t}_c\right) = \tilde{T}_{max,\,ss}\,. \qquad (14)$$

At t = 0, the uniform heat flux q″ lands on the left wall (Fig. 1), the tree channels are filled with stagnant coolant, and the remaining boundaries are adiabatic. At t = t_d, the pressure difference Be is applied. The coolant begins to flow, and gradually changes to fully developed flow. The time delay before the start of the flow of coolant is set in relation to t_c, as a fraction of the time constant determined in Eq. (14),

$$\tau = \frac{\tilde{t}_d}{\tilde{t}_c} \qquad (15)$$

As shown in Fig. 8, when the relative time delay τ is larger than a critical value (called τ_*), the peak temperature overshoots the steady-state level. It is assumed that the solid material and its functions can withstand the steady-state peak temperature, but fail when the hot-spot temperature exceeds the steady-state peak temperature. The allowable peak temperature is the peak temperature under steady-state conditions. Therefore, the critical time delay τ_* is a measure of the longest delay time within which the vascular structure remains safe.

Figure 8 shows the evolution of the peak temperature when a time delay exists. During the delay time there is no flow and the hot-spot temperature rises rapidly. When the coolant begins to flow, the rise of $\tilde{T}_{max}$ stops, and the trend is reversed. The horizontal dashed line shows the level of the steady-state peak temperature, or the allowable peak temperature. When the time delay τ is equal to or less than approximately 1, the transient peak temperature is kept under the allowable level. When τ is greater than 1, overheating occurs. In conclusion, for the design studied in Fig. 8 the critical delay is $\tau_* \cong 1$, and this means that in this case t_d is essentially equal to t_c.

Figure 9 shows the temperature distribution on the heated side of the wall (the left side in Fig. 7a), on only the upper half of the surface, i.e. in the vicinity of the upper eight outlets. Immediately after the start of cooling (at $\tilde{t}_d + 6\times10^{-5}$), the hot spots are concentrated in two places, between the upper two outlets and between the lower two, although the upper hot spot is the hottest. A little later ($\tilde{t}_d + 1.2\times10^{-4}$) the hot spots jump outside the dendrite, above the upper outlet, and below the lower outlet. This time the hottest spot is the lower hot spot because of a difference in mass flow rates: the flow rate through the uppermost outlet exceeds by 7.3% the flow rate through the lowest outlet.

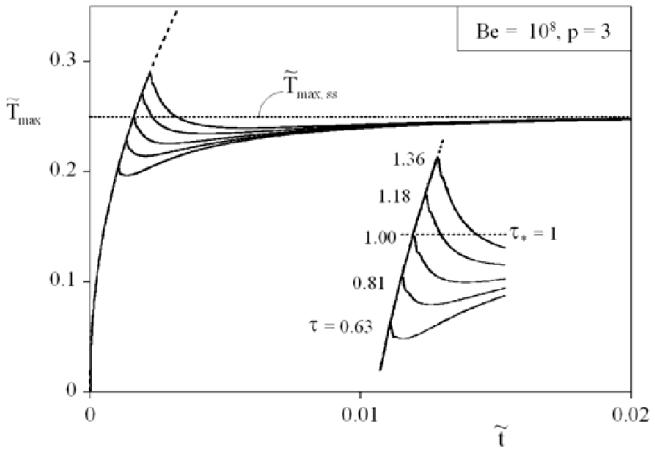

Figure 8 The effect of the time delay τ on the peak temperature when Be = 10^8 and p = 3 [4].

VASCULAR COMPOSITES COOLED WITH GRIDS AND RADIAL CHANNELS

Two additional configurations were explored: grids and (b) radial channels, Fig. 10 [5]. Two characteristic times are defined to assist in the evaluation – the characteristic response time $\tilde{t}_{ss}$ and the heat removal time ε, σ. The vascularized composite body is a square slab of size L×L and thickness 0.1L, which is heated from the bottom with a uniform heat flux q″. The other surfaces are adiabatic. Cooling is provided by an embedded three-dimensional channel network. The spacing between ports on the perimeter is fixed ($L_g = L_r$). The channel thicknesses of the grids and radial patterns are d_g and d_r, respectively. Figure 11 shows the embedded channels in greater detail, in only one eighth of the slab. The patterns of isotherms displayed in Figs. 10 and 11 are for the steady state.

Two flow directions are considered, from the center of the slab to the periphery and from the periphery to the center. In total, four flow configurations were explored:

GI: grids with inlet in the center
GO: grids with outlet in the center
RI: radial channels with inlet in the center
RO: radial channels with outlet in the center

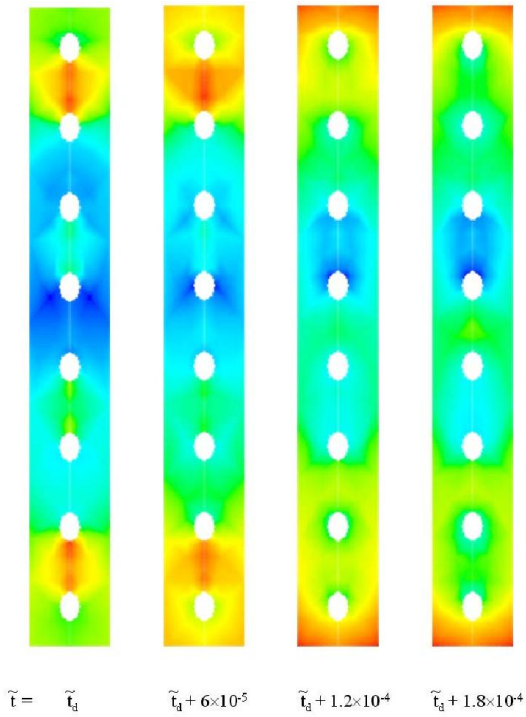

Figure 9 The migration of the hot spots after the coolant starts flowing: the temperature distribution on the heated (left) side in Fig. 7a (p = 3), in the vicinity of the upper eight outlets [4].

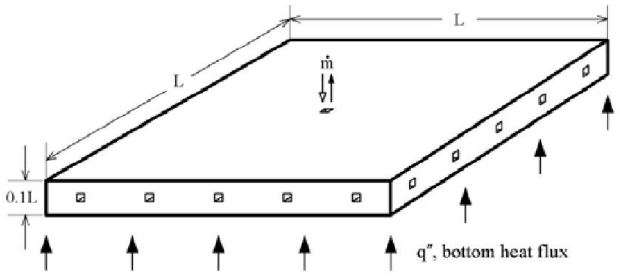

Figure 10 Slab heated with uniform flux from below: (a) Grid channels, (b) Radial channels. Steady state temperature distributions in the middle planes of the slabs ($Be = 10^{10}$)[5].

Several quantities were fixed: the volume of the slab V, the total volume of the flow channels V_f (or the porosity $j = V_f/V$), and the pressure difference between the inlet and the outlet (ΔP).

In practice the implementation of vascular cooling also requires a system of sensing the start of uniform heating at $\tilde{t} = 0$, and then triggering the pumping of coolant. At $\tilde{t} = 0$, the heat flux q'' is applied on a slab that is not bathed by the coolant (the channels are filled with stagnant coolant). At $\tilde{t} = \tilde{t}_d$, the coolant starts to flow and, in time, the flow approaches a fully developed flow. The cooling performance of flow configurations can be evaluated by monitoring their temperature distribution and hot volume fraction, which is defined as

$$\sigma = \frac{V_{hot}}{V} \tag{16}$$

where V_{hot} is the volume of material with temperatures between $\tilde{T}_{max}$ and $\tilde{T}_{hot}$ $\left(\tilde{T}_{hot} < \tilde{T} < \tilde{T}_{max}\right)$ such that $\tilde{T}_{hot}$ approaches $\tilde{T}_{max}$ within 10 percent,

Here we illustrate the distribution of the hot volume (the solid volume σ_s and the fluid volume σ_f) of each configuration when the transient simulations reach steady state. The hot volume fractions σ_s and σ_f are determined by substituting local values of $\tilde{T}_{max}$ $\tilde{T}_{min}$ and $\tilde{T}_{hot}$ in the solid and fluid domains. The hot volume fraction of the solid domain are shown in Fig. 12. We see that when Be is smaller than 10^{10} the designs with outlet in the center have smaller σ_s values than the designs with inlet in the center. Smaller σ_s values are more advantageous for the safe operation and mechanical worthiness of the solid structure. Figure 12 also shows that the choice between grids and radial channels is minor. The more effective way to reduce the hot volume fraction is to orient the flow from the periphery to the center (GO and RO). The hot volume fractions in the fluid domain has a behavior similar to the one shown in Fig. 12. The transient performance of grid and radial designs with time delay is documented further in Ref. [5].

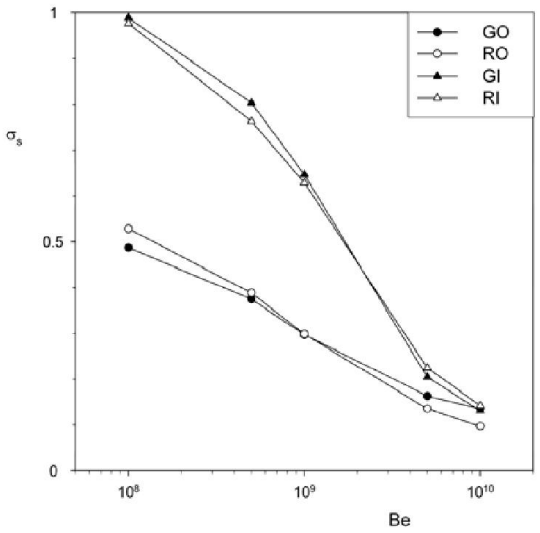

Figure 12 The hot volume fraction of the solid domain of four configurations at five Be values [5].

Figure 11 One eighth of a square slab with embedded channels: (a) Grid channels, (b) Radial channels. The center of the slab is in the upper-left corner. Steady state temperature distributions over the surfaces of the bottom half of the slab ($Be = 10^{10}$) [5].

CONCLUSION

In this paper we reviewed our group's progress on the transient cooling performance of vascular bodies subjected to sudden heating and cooled with single-phase coolant [3-5]. A time delay separates the start of heating from the initiation of coolant flow. The chief objective was to determine the largest

permissible time delay so that the hot spot temperatures do not overshoot the maximum allowable limit.

The overriding conclusion is that the configuration of the vascular architecture is essential to insuring the high level of performance of the vascular material. This is in complete accord with the method of design with constructal theory [1, 12]. When the applied pressure difference is specified, there is a certain design that offers better cooling (e.g., Fig. 3) and larger allowable delay time (e.g., Fig. 6).

This fundamental aspect is important, because it orients the entire field of design toward "sculpting" the flow configurations so that they perform better and better in a global sense [1, 2, 12]. Here we identified this opportunity even more sharply by focusing on the transient response of the designed architectures.

Acknowledgment. This research was supported by the Air Force Office of Scientific Research.

REFERENCES

[1] A. Bejan and S. Lorente, Design with Constructal Theory, Wiley, Hoboken, 2008.

[2] A. Bejan, Advanced Engineering Thermodynamics, 2nd ed., Wiley, New York, 1997.

[3] J. Lee, S. Lorente and A. Bejan, Transient cooling of smart vascular materials for self-cooling, J. Appl. Phys. (2009) 064904.

[4] S. Kim, S. Lorente and A. Bejan, Transient behavior of vascularized walls exposed to sudden heating, Int. J. Thermal Sciences 48 (2009) 2046-2052.

[5] K.-M. Wang, S. Lorente and A. Bejan, The transient response of vascular composites cooled with grids and radial channels, Int. Heat Mass Transfer 52 (2009) 4175-4183.

[6] S. Lorente, A. Bejan, Heterogeneous porous media as multiscale structures for maximum flow access, J. Appl. Phys. 100 (2006) 114909.

[7] S. Lorente, W. Wechsatol, A. Bejan, Tree-shaped flow structures designed by minimizing path lengths, Int. J. Heat Mass Transfer 45 (2002) 3299-3312.

[8] S. Lorente, A. Bejan, Svelteness, freedom to morph, and constructal multi-scale flow structures, Int. J. Thermal Sci. 44 (2005) 1123-1130.

[9] A. H. Reis, Constructal theory: from engineering to physics, and how flow systems develop shape and structure, Appl. Mechanics Reviews, 59 (2006) 269-282.

[10] S. Bhattacharjee, W. L. Grosshandler, The formation of a wall jet near a high temperature wall under microgravity environment, ASME HTD, 96 (1988) 711-716.

[11] S. Petrescu, Comments on the optimal spacing of parallel plates cooled by forced convection, Int. J. Heat Mass Transfer 37 (1994) 1283.

[12] A. Bejan and S. Lorente, Constructal theory of generation of configuration in nature and engineering, J. Appl. Phys. 100 (2006) 041301.